

# Theoretical study on a reaction pathway of Ziegler-Natta-type catalysis<sup>a)</sup>

O. Novaro<sup>b)</sup> and E. Blaisten-Barojas

*Instituto de Física, Universidad Nacional Autónoma de México, Apartado Postal 20-364, México 20, D.F.*

E. Clementi and G. Giunchi

*Montedison, S.p.A., Istituto Ricerche "G. Donegani," Via Fauser 4, Novara, Italia*

M. E. Ruiz-Vizcaya

*Instituto Mexicano del Petróleo, Av. de los Cien Metros 152, México 14, D.F.*

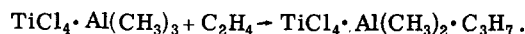
(Received 8 July 1977)

*Ab initio* SCF-LCAO-MO all-electron calculations have been performed for the catalyzed reaction, related to the Ziegler-Natta polymerization process  $\text{TiCl}_4 \cdot \text{Al}(\text{CH}_3)_3 + \text{C}_2\text{H}_4 \rightarrow \text{TiCl}_4 \cdot \text{Al}(\text{CH}_3)_2 \cdot \text{C}_3\text{H}_7$ . The energy of the Ti-Al-ethylene complex during the reaction pathway is associated to the following processes: First, the ethylene coordinates to the catalyst complex and subsequently it reacts with the methyl moiety producing an activation energy barrier mainly due to the breaking of the ethylene double bond. The computed barrier height (15 kcal/mole) is in reasonable agreement with experimental activation energies. The identification of the energy barrier is based on the analysis of the electron population, bond energies, and molecular orbitals of the system as they evolve during the reaction. A comparison with the qualitative picture resulting from the classical model of Cossee and with semiempirical calculations is presented. From these calculations a model is derived which leads to a tentative suggestion for the enhancement of the catalytic activity. We consider this suggestion (regardless of its practical value), as well as the model, as examples of the type of theoretical results that can be furnished by quantum mechanics.

## I. INTRODUCTION

For people involved in the practical aspects of catalysis, the basic role played by a catalyst is to modify the reaction rate of the process by lowering certain activation barriers and consequently augmenting the selectivity with respect to certain products. In other words, catalysis chemists are primarily interested in *changes*, and in attempting a theoretical approach to the catalytic phenomenon it is good to keep this in mind. To give a long list of eigenvalues for a static organometallic complex, for instance, would be of interest mostly for comparison with spectroscopic data or with other theoretical studies, but only indirectly related to the mechanism of a catalytic reaction. To go to the heart of the problem theoretically, one has to analyze the evolution of the process, attempting to understand the role played by the catalyst during the reaction.

Here we present one of the first attempts to perform a fully *ab initio* study of a reaction pathway at an assumed catalyst site. The nature of the present work is an all-electron *ab initio*, restricted Hartree-Fock study, composed of a sequence of calculations on different configurations of the reactant-catalyst system purported to represent the evolution of the process



Although we have chosen a process likely to be intimately connected with Ziegler-Natta polymerization,<sup>1,2</sup> we believe that our results may have a bearing to models for

catalysis in general. Indeed, *first*, we discuss a chain growth mechanism that can be considered a typical repeating reaction for the polymerization process; *second*, we select a model for a catalytic site which can be related to homogeneous or heterogeneous catalysts. Furthermore, the quantum mechanical character of these calculations gives insight to the nature of the catalytic phenomenon by providing us with various tools for its analysis.

These "tools" are in fact successively discussed in the different sections of this paper. The evolution of the total energy of the system gives the quantum mechanical information related directly to experimental data. In Sec. II we present the total energy analysis and also the net atomic charges as they change through the reaction pathway (leading from the ethylene approach to the titanium site to the "polymerization" reaction, i.e., the hydrocarbon chain growth). The activation barrier resulting from this study is of the right order of magnitude, although a more thorough study of the potential energy surface would evidently be desirable.

Less directly related to experimental data, but of great value to visualize *chemical changes*, is the information about the eigenvectors and eigenvalues given in Sec. III. In this section the description of all of the molecular orbitals as they change during the evolution of the process is given, showing that it is an oversimplification to assign to a few orbitals only the determinant role for the whole catalytic action. Also, hypotheses such as singling out one (or a few) atom as "active site" appear somewhat dangerous in the light of the information of Sec. III, where the electronic delocalization at certain stages of the reaction is so notable that the olefin should perhaps be considered to be interacting

<sup>a)</sup>Work supported in part by Fondo Elena Aizen de Moshinsky and Programa Nacional de Ciencias Básicas, CONACYT.

<sup>b)</sup>Consultant at the Instituto Mexicano del Petróleo, México.

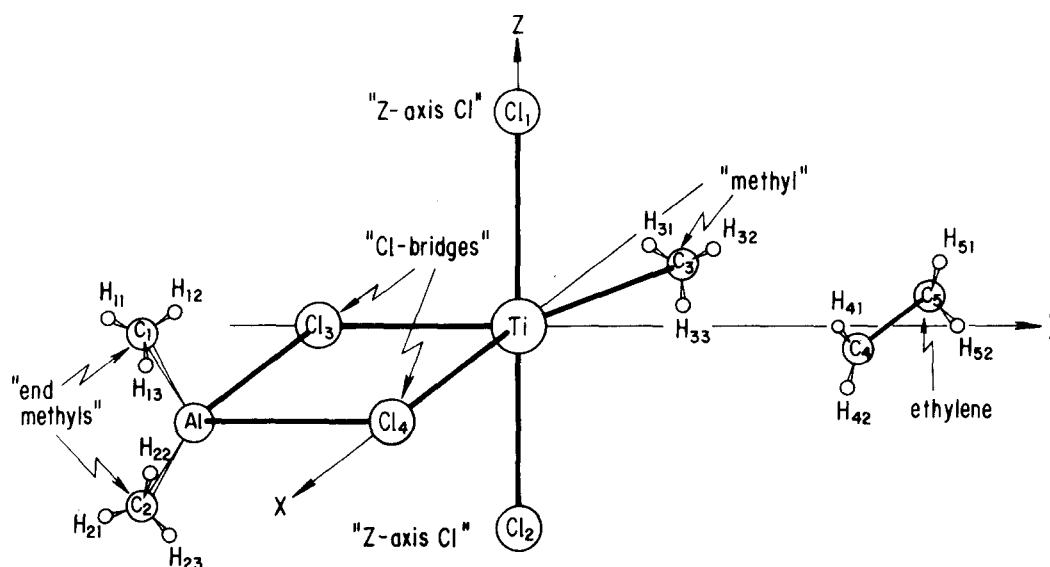


FIG. 1. Schematic representation of the catalyst–ethylene complex. The adopted convention for the notation of single atoms or group of atoms is evidenced.

with even the farthest removed parts of the catalyst complex.

In Sec. IV another tool is used to once again analyze the reaction pathway. This is done by a bond energy analysis both for individual atom–atom interactions and for interactions between certain groups of atoms. An independent viewpoint on the chemical reaction is derived from the results presented in Secs. II–IV. However, it is interesting to see that these viewpoints not only do not conflict but complement each other well, composing a model of the catalytic process. This model is compared in Sec. V with other theoretical descriptions for the Ziegler–Natta process. In particular the well-known Cossee model<sup>3</sup> is corroborated partly by some of the information from the complete *ab initio* study, which, however, gives a richer and more complex picture of the process. In this same section a somewhat tentative discussion of the contributions that studies such as this one can make to solve practical questions of catalysis, is also given. Finally, in Sec. VI some concluding remarks are presented.

The present calculation uses a set of 271 Gaussians (specified in Appendix A) contracted into 99 and the IBMOL program.<sup>4</sup>

## II. REACTION PATHWAY

In this section we shall study the electronic structure of the titanium–aluminium–ethylene complex as it evolves in a sequence of 12 steps, whereby the ethylene first enters the coordination sphere of the catalytic complex and then inserts into the titanium–methyl bond. Therefore, an analysis of the total energy and charge distribution at the different steps of the process provides a guide for understanding the dynamics of the reaction. Clearly, in a complex reaction there are a large number of possible pathways; here we have selected the one we feel is most significant and likely very near to the minimum energy path.

The structure of the catalytic complex interacting with the ethylene is given in Fig. 1. This geometry has been discussed elsewhere,<sup>5</sup> and in Appendix B we add some details on the variations of some of the geometrical parameters of the system. The optimization of these variables, although far from being complete, gives us a way to guess a probable approach of the olefin to the catalyst along a defined direction. In Fig. 1 we establish a few conventions to identify the different atoms and regions in the catalyst. There are three methyl groups and four chlorine atoms playing quite different roles in the reaction. Henceforth, whenever the “methyl” is mentioned we shall always refer to the titanium coordinated methyl, i. e., the one associated to the chain growth process, whereas the two other methyl groups, coordinated to the aluminium, will be referred as the “end-methyls.” The two chlorines in the  $xy$  plane bonded to Ti and Al will be called the “Cl bridges,” (to emphasize their role in the delocalized bonding between the metals), the corresponding region spanned by the metals and Cl bridges, will be referred to as the “bridged structure.” Finally the other chlorine atoms coordinated, in our model, solely to the titanium will be called the “z axis Cl’s.”

In Table I we report the geometries and relative energies of a sequence of steps that start with the coordination of an incoming ethylene (steps 1–5) continues with the ethylene’s  $\pi$  bond breaking (steps 4–8) and ends with its reaction with the methyl to produce the chain growth, that represents a model for the first phase of a polymerization process (steps 8–12). In Figs. 2 and 3 we present a pictorial representation of the changes during the process: of the complex–reactant geometries (Fig. 2) and of the corresponding total energies (Fig. 3). The information is supplemented by the atomic net charges of Table II. Notice in this table that during the reaction evolution the complex contains strongly polar atoms, both metal atoms having high positive charges. Even if it is known that small basis sets overestimate the polarity, we are of the opinion that the polarity pic-

TABLE I. Molecular configurations and total energies of a sequence of steps describing the reaction pathway. Total energies are measured with respect to the first step energy  $E_1 = -3112.1681$  a.u. For the definition of the parameters see Appendix B.

Reaction steps	$R(\text{Ti}-\text{C}_4)$ (Å)	$R(\text{Ti}-\text{C}_5)$ (Å)	$R(\text{Ti}-\text{C}_3)$ (Å)	$R(\text{C}_3-\text{C}_5)$ (Å)	$\alpha_R$ (°)	$\alpha_0$ (°)	$\alpha_I$ (°)	$r$ (Å)	$\Delta E = E_i - E_1$ (kcal/mole)
1	7.03	7.03	2.15	5.55	45	0	117	1.337	0
2	5.04	5.04	2.15	3.58	45	0	117	1.337	-0.3
3	4.06	4.06	2.15	3.23	28	0	117	1.337	-1.9
4	3.08	3.08	2.15	2.71	13	8	115	1.383	-4.2
5	2.59	2.59	2.15	2.70	8	16	115	1.383	-3.0
6	2.40	2.43	2.15	2.69	0	19	114	1.406	5.3
7	2.24	2.39	2.26	2.48	-2.3	23	113.25	1.428	15.0
8	2.18	2.49	2.37	2.31	-4.6	28	112.49	1.451	10.9
9	2.14	2.60	2.48	2.14	-6.9	34	111.74	1.473	1.1
10	2.124	2.73	2.59	1.95	-9.2	40.9	110.98	1.495	-14.2
11	2.126	2.88	2.65	1.75	-11.5	47.8	110.23	1.518	-34.5
12	2.15	3.03	2.81	1.54	-13.8	54.7	109.47	1.54	-40.3

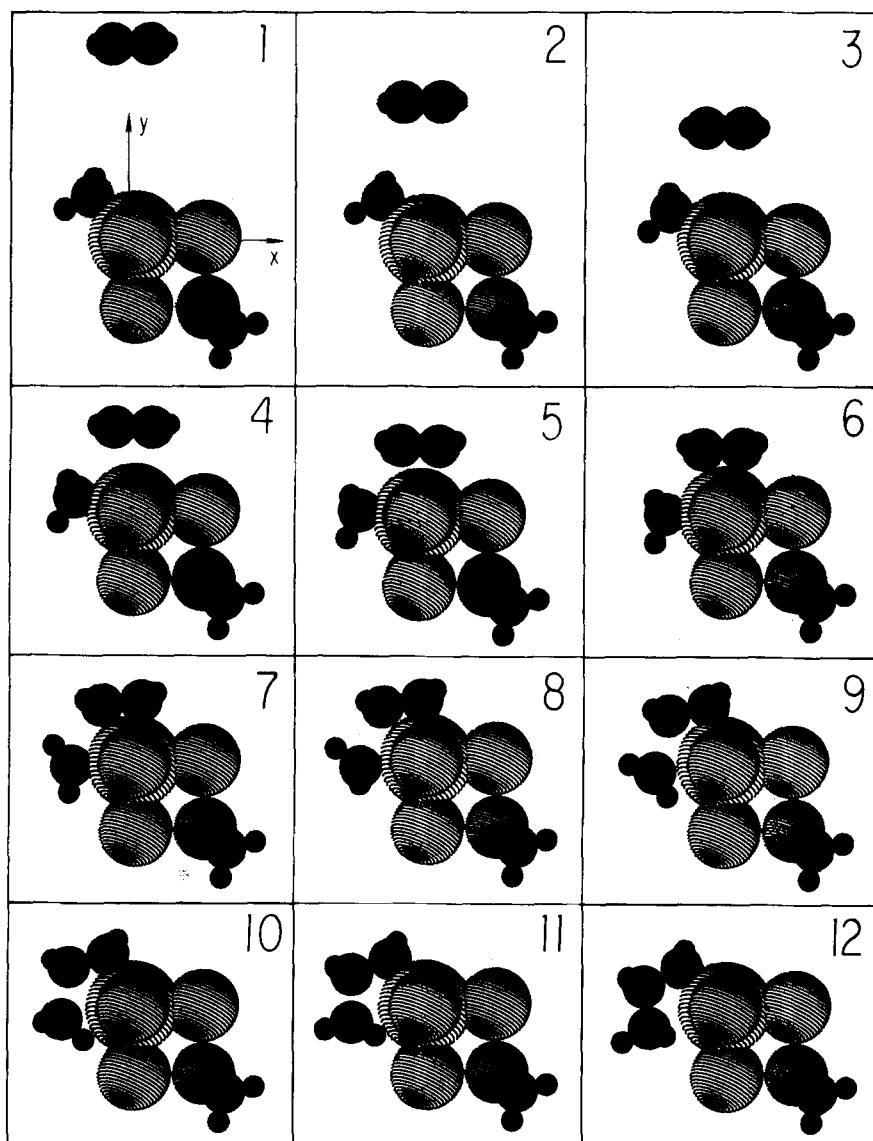


FIG. 2. View of three-dimensional models in the  $XY$  plane for the conformations of the twelve reaction steps. Additional information on the geometries are given in Table I and in the text. This figure was obtained using a program developed by E. Aguilar of Instituto Mexicano del Petróleo.

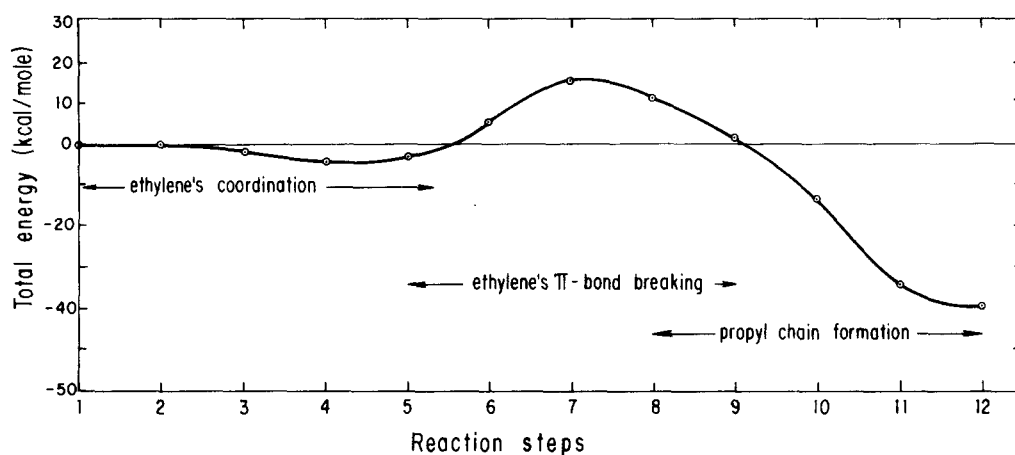


FIG. 3. Evolution of the total energy of the catalyst–ethylene complex during the reaction.

ture will not change substantially with the use of a larger basis set.

Figure 3 shows an initial shallow minimum for the coordination of the ethylene, followed by an important activation barrier, and finally a notable energy stabilization of the system. The height of the barrier is not exceedingly large and compares reasonably well with experimental data. From the original activation energy reported by Natta and Pasquon<sup>6</sup> (10 kcal/mol) for the heterogeneous catalyst to very recent results for Ziegler-type dimerization processes<sup>7</sup> (with activation energies between 12.5 and 16 kcal/mol), and including also results for homogeneous Ti–Al catalytic complexes<sup>8</sup> (activation energies of 8–12 kcal/mol) one can see that the present value (of the order of 15 kcal/mol) is of the right order of magnitude even if somewhat high. We realize, of course, that our model for the catalyst cannot be considered a realistic representation of all these different reactions.

The energy lowering observed in steps 4–6 (Fig. 3)

is a consequence of the formation of a new Ti–ethylene coordination bond. During the ethylene's entrance into the titanium coordination sphere, however, a methyl–ethylene repulsion immediately appears, as shall be shown later on (Sec. IV). The balance between the energy gain from coordination and the loss from this repulsion is quite delicate. In Appendix B it is shown in fact, that during this part of the process the minimal energy pathway follows a deep “gorge” with steep walls. Consequently, if the methyl wouldn't be able to move (towards the  $-x$  axis in Fig. 1) during the ethylene's approach, an important activation barrier would ensue. Notice that at steps 4 and 5 the methyl and ethylene positions are such that the complex acquires a *quasi*octahedral symmetry.

The energy barrier in Fig. 3 is associated with important chemical changes within the complex. It is during this part of the reaction that the ethylene  $\pi$  bond effectively admixes with the coordination complex and finally breaks, after step 8. Thereafter, the energy of the system steadily decreases until the propyl chain is

TABLE II. Atomic net charges of the titanium–aluminum–ethylene complex. All numbers stand for the difference between the atomic number and the calculated number of electrons in each center of the complex.

Reaction steps	Atoms not changing position during the reaction								Atoms varying their position		
	C <sub>1</sub>	C <sub>2</sub>	Al	Cl <sub>3</sub>	Cl <sub>4</sub>	Cl <sub>1</sub>	Cl <sub>2</sub>	Ti	C <sub>3</sub>	C <sub>4</sub>	C <sub>5</sub>
1	-0.95	-0.95	1.25	-0.41	-0.41	-0.56	-0.56	2.31	-0.97	-0.39	-0.39
2	-0.95	-0.95	1.25	-0.41	-0.41	-0.56	-0.56	2.30	-0.97	-0.40	-0.39
3	-0.95	-0.95	1.25	-0.41	-0.41	-0.56	-0.56	2.30	-0.93	-0.43	-0.36
4	-0.95	-0.95	1.25	-0.40	-0.40	-0.56	-0.56	2.31	-0.92	-0.49	-0.40
5	-0.95	-0.95	1.25	-0.40	-0.40	-0.56	-0.56	2.34	-0.94	-0.53	-0.44
6	-0.95	-0.95	1.25	-0.39	-0.43	-0.57	-0.57	2.35	-0.95	-0.56	-0.48
7	-0.95	-0.95	1.25	-0.40	-0.41	-0.56	-0.56	2.35	-0.90	-0.66	-0.44
8	-0.95	-0.95	1.25	-0.41	-0.40	-0.56	-0.56	2.36	-0.84	-0.73	-0.40
9	-0.95	-0.95	1.25	-0.43	-0.40	-0.56	-0.56	2.36	-0.77	-0.76	-0.39
10	-0.95	-0.95	1.25	-0.42	-0.39	-0.56	-0.56	2.35	-0.67	-0.77	-0.39
11	-0.95	-0.95	1.25	-0.42	-0.40	-0.56	-0.56	2.33	-0.61	-0.77	-0.39
12	-0.95	-0.95	1.25	-0.41	-0.40	-0.56	-0.56	2.31	-0.60	-0.76	-0.40

completely formed and coordinated at the Ti site. The effects of these chemical changes are reflected in the charge distributions of Table II. Notice, for instance, that at the earlier stages (steps 2–6) the ethylene carbons begin to build up their already high negative charge. So much so that after the barrier is surmounted (steps 9–12) the charge in  $C_4$  already surpasses the charge in  $C_3$ , therefore reflecting a stronger interaction between the Ti and the olefin carbon than between Ti and the methyl. During the last part of the process the charge in  $C_5$  remains constant.

Let us summarize the characteristics of the reaction coordinate not only as given from the total energy, but also using information discussed in the following sections. When the ethylene approaches the catalyst a new coordination bond is formed at the Ti site; this gives origin to the first shallow minimum. Suppose that the reaction would take place between free molecules of ethylene and methane. Then their approach would imply a mere scattering of the molecules by a collision. In fact, many collisions at very high temperatures would be necessary to make the molecules react. On the other hand, suppose that the methyl group would be strongly attached to the titanium site. The directional character of this bond would not allow the methyl to relax from its position and accept the ethylene. Compare these two pictures with the situation obtained from our results (see Appendix B and Secs. III and IV). First, the ethylene repels the methyl, but the labile character of the Ti–methyl bond (active rotational mode) allows the methyl to reach a different and energetically favorable position. Then, the reaction with ethylene begins and proceeds without ever breaking away from the Ti site, as seen in Fig. 2. The activation barrier is associated to the breaking of two bonds, the ethylene double bond and the Ti–methyl coordination bond. The height of this energy barrier is, in fact, surprisingly small for the breaking of a double bond, which for an isolated ethylene would be much higher. We anticipate here the reasons, namely (i) the ethylene is already inside the catalyst coordination sphere, and (ii) the new bonds Ti– $C_4$  and  $C_5$ – $C_3$  begin to build up when the  $C_4$ – $C_5$  double bond actually breaks. Once the new bonds are formed, the energy of the entire complex goes down smoothly.

The results and therefore the model reported here are qualified as follows: First, all calculations were done using a nearly minimal basis set, not having yet fully tested the effects of the basis set size. A somewhat extended set (including one extra  $3d$  function) has been used<sup>5</sup> in a preliminary study indicating that the main energy trend remains essentially constant. Likely, however, more attention should be given to this point, even if it requires to perform even heavier computations than those here given. Secondly, electron correlation effects were not included; however, as the number of bonds is constant through the reaction, correlation effects may not be crucially important. Finally, as we have not fully studied the whole potential energy surface, the present results serve to present an approximate description of one among several alternative possible pathways for the process. Even at this stage, however, this study

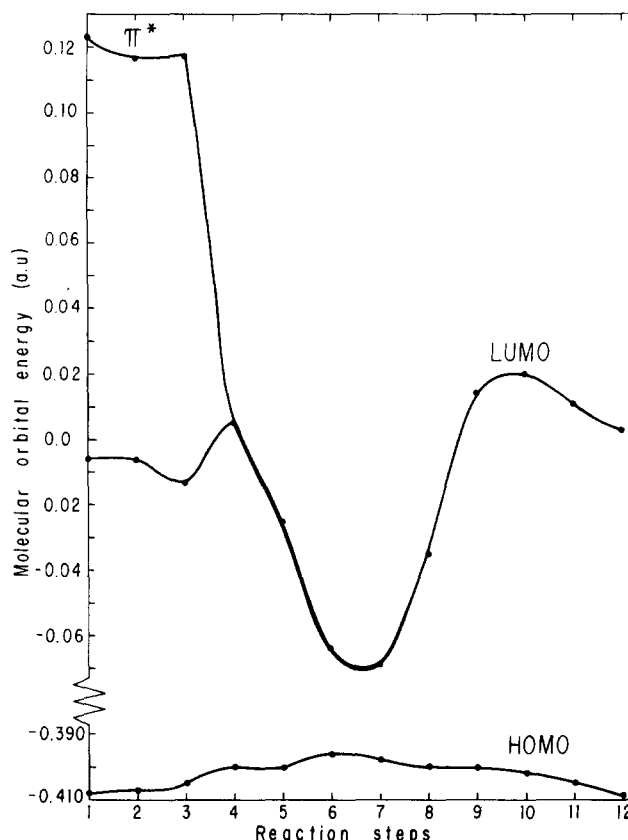


FIG. 4. Orbital energies of the HOMO (MO 73), LUMO (MO 74), and of the  $\pi^*$ -virtual orbital. The latter loses its identity after step 8, as emphasized by fading of the heavy line.

does provide a first approach to the understanding of the quantum mechanical aspects of a catalytic process.

### III. MOLECULAR ORBITAL STRUCTURE

In any SCF calculation only the *total* wavefunction and the *total* energy have well defined physical meaning. Nevertheless, the information that one can obtain from the molecular orbitals of the system provides additional insight to the process. Here we analyze the molecular orbitals (MO's) as they change during the reaction in order to see how they reflect the chemical evolution. We recall that in our system there are 146 electrons described by 73 occupied MO's, constructed as linear combinations of 99 contracted Gaussian functions.

In Table III we present the most notable features of all 99 MO's. The contents of Table III are qualitative, however, the complete tables of MO's are available elsewhere.<sup>9</sup> From Table III we see that several occupied orbitals reflect in different ways the chemical changes of the process. Obviously, not all MO's have equal sensitivity nor play equal roles during the process. Thus, italics are used to emphasize particularly important aspects of the MO structure.

Let us analyze in detail two particularly revealing MO's namely the so-called HOMO and LUMO, the highest occupied and the lowest unoccupied molecular orbitals, respectively. Usually, the justification for singling out these orbitals is the possibility of a thermal population flow from one to the other. However, as can be seen in Fig. 4 the energy gap between them is of the or-

TABLE III. Character and evolution of the MO structure of the Ti-Al-ethylene complex through the reaction pathway of Fig. 3. The MO's are ordered with increasing energies.

MO	Ethylene's coordination	Ethylene's $\pi$ -bond breaking	Propyl chain formation
1-39	Inner shell MO's. These orbitals suffer no modifications during the reaction.		
40	Ethylene $\sigma$ bond	Ethylene $\sigma$ bond slightly destabilized during the 2nd activation barrier. Gradual incorporation of the C <sub>3</sub> <i>s, p</i> functions. Titanium <i>s, p, d</i> marginal contributions.	MO restabilized. C <sub>3</sub> is fully incorporated in the $\sigma$ bonds of the whole propyl chain. Titanium contributions stay constant.
41-42	Associated to the Cl's bridges	No changes	No changes
43-44	<i>s</i> function contributions from Cl <sub>1</sub> , Cl <sub>2</sub> , Ti, and C <sub>3</sub>	Same character with gradual incorporation of <i>s</i> functions of C <sub>4</sub> and C <sub>5</sub> .	<i>s</i> functions from Cl <sub>1</sub> , Cl <sub>2</sub> , Ti, C <sub>4</sub> , C <sub>5</sub> , and C <sub>3</sub> .
45	<i>s</i> functions in Cl <sub>1</sub> and Cl <sub>2</sub>	No changes	No changes
46-47	Localized solely in the end methyls	No changes	No changes
48-51	Internal C-H bonds in ethylene: one $\sigma$ bonding and one $\sigma$ antibonding in C-C axis, two perpendicular to this axis.	Inclusion of methyl C-H bonds	C-H bonds in the propyl chain. The bonding and antibonding MO's extend to all propyl $\sigma$ bonds.
52	Originally C-H bond within methyl	<i>Notable energy stabilization. <math>\pi</math> bond in ethylene appears through the admixing of C<sub>4</sub> and C<sub>5</sub>, <i>p<sub>y</sub></i> functions. Also, 3<i>p<sub>y</sub></i>, 3<i>d<sub>y<sup>2</sup></sub></i></i> contributions from Ti.	Looses its $\pi$ bond character and becomes $\sigma$ bond within propyl chain. Also contributing to Ti-propyl coordination.
53	Largely localized in Al, end-methyls, and Cl's bridges.	<i>Total delocalization spanning from Al to the ethylene and methyl carbons</i>	After second activation barrier MO is again localized in the Al region.
54	C-H bonds within the methyl	Gradual incorporation of ethylene	C-H bonds on the whole propyl chain
55-58	C-H bond within the end-methyls	No changes	No changes
59	Highly localized in the ethylene	<i>Notable energy stabilization. Total delocalization spanning from the methyl to the Al region.</i>	Regains its localization now within the propyl chain.
60-62	The most important Ti <i>s</i> and <i>d</i> contributions, also <i>p</i> functions from bridging Cl's. These directed towards Cl <sub>1</sub> , Cl <sub>2</sub> , Al, and C <sub>3</sub> .	<i>Same as before, but Ti <i>d<sub>y<sup>2</sup></sub></i> function overlapping with ethylene's <math>\pi</math> bond.</i>	Ethylene's double bond broken. These MO's are again Ti directed bonds towards Cl <sub>1</sub> , Cl <sub>2</sub> , Al, and C <sub>4</sub> in the propyl chain.
63-66	Localized in the Cl-bridged region. Same directionality as MO's 60-62.	<i>Incorporation of ethylene's <math>\pi</math> bond.</i>	Same as in early stages but C <sub>4</sub> replacing C <sub>3</sub> .
67	<i>Pure ethylene <math>\pi</math> bond.</i>	Acquires the same nature as MO's 63-66. Slight asymmetry between the C <sub>4</sub> and C <sub>5</sub> <i>p<sub>y</sub></i> contributions	Same as MO's 63-66. Contributes to propyl $\sigma$ bonds. <i>The <math>\pi</math> bond is gone.</i>
68-72	Mainly localized in Cl <sub>1</sub> and Cl <sub>2</sub> . Admixing of the bridging Cl's and the methyl carbon C <sub>3</sub>	Incorporation of the ethylene $\pi$ -bond.	Same as in early stages but C <sub>4</sub> replaces C <sub>3</sub> .
73	Highest occupied MO (HOMO). <i>Highly directional contributions from Ti (dominated by <i>d<sub>xy</sub></i> function) determinantly overlapping with <i>sp</i> hybrid from C<sub>3</sub></i>		
74	Lowest unoccupied MO (LUMO). Antibonding orbital for Ti-methyl	See discussion of its evolution in the text and Fig. 4.	
75-78	Empty <i>d</i> -orbitals in Ti	No changes	No changes
79	Antibonding MO in ethylene's double bond $\pi^*$	See discussion of its evolution in the text and Fig. 4.	
80-99	Mostly antibonding contributions to C-H bonds, metal-Cl bonds, etc.	No changes	No changes

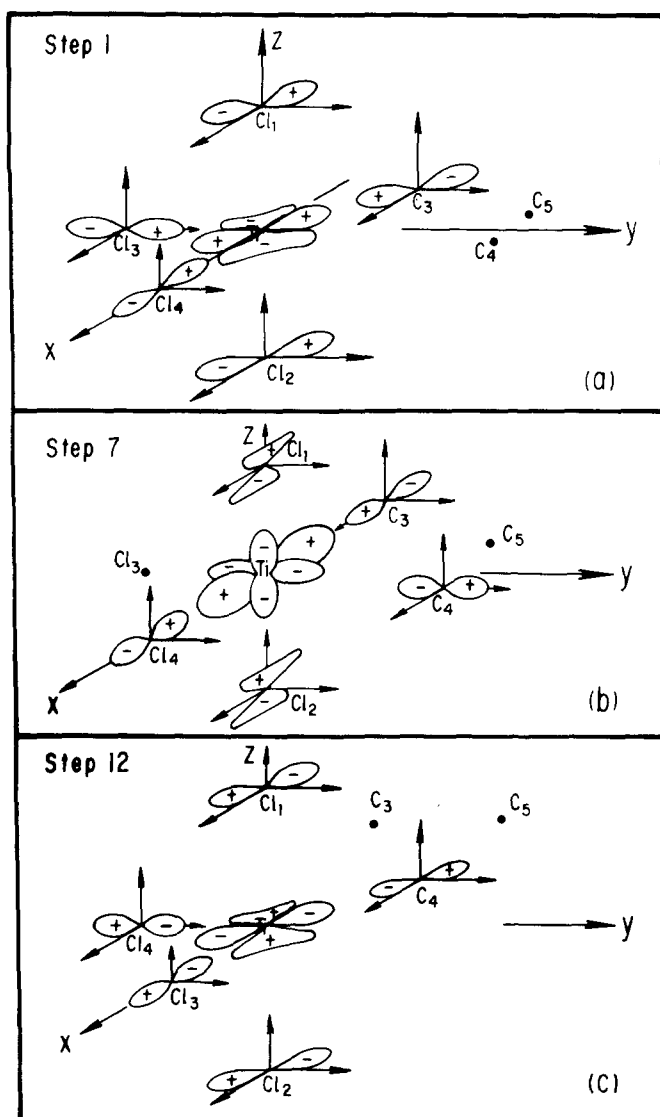


FIG. 5. Schematic representation of the atomic orbital contributions to the HOMO at three characteristic stages of the reaction.

der of 0.3–0.4 a. u., and consequently this is a forbidden event. On the other hand, we must also remember that if an attempt would be made to introduce electron correlation effects, then the lowest unoccupied orbital would certainly participate with a nonnegligible weight.

The HOMO, as Table III shows, at the early stages of the reaction has dominant contributions from Ti ( $4s$  and  $3d_{xy}$ ) and from the methyl carbon ( $1p_x$  and  $2p_y$ ), which are overlapping positively. It also has  $3p_x$  and  $3p_y$  contributions from the chlorine bridges. All this is schematized in Fig. 5(a), which emphasizes that this MO is associated to the Ti–methyl bond at the beginning of the reaction. When the ethylene approaches the Ti site, the situation changes gradually, causing this MO to be slightly destabilized energetically (see Fig. 4). It is restabilized during the propyl chain formation when the  $C_4$  in ethylene begins to admix. Figure 5(b) gives the HOMO when this admixing begins (step 7) showing the directionality loss of the Ti contribution which is now interacting with both  $C_3$  and  $C_4$ . At the very last steps

of the reaction  $C_4$  has completely replaced  $C_3$  in this MO, as shown in Fig. 5(c). The HOMO becomes again the alkyl bonding orbital recovering its original energy (Fig. 4).

Now let us discuss the nature of the LUMO, namely, the virtual MO 74. As stated in Table III, at the earliest stages this MO is basically an antibonding MO between the Ti site and the methyl due to the negative overlap between the Ti  $d$  orbital with the  $C_3$   $p$  functions. The discussion of the evolution of the LUMO necessarily brings in MO 79, identified in Table III as the ethylene  $\pi^*$  orbital. The energies of these two orbitals are depicted in Fig. 4. From it the drastic stabilization of  $\pi^*$  orbital and its admixture with the LUMO is evident. This effect is reflected on the LUMO structure as shown in Fig. 6; it is now (at step six) basically composed of the  $p_y$  functions from the carbons in ethylene overlapping positively with two lobes of the Ti- $d_{xy}$  orbital. Thus, the titanium plays a crucial role for the ethylene coordination and subsequent double bond breaking. Notice that the energy minimum reached by the  $\pi^*$ -LUMO orbital in Fig. 4 corresponds to the top of the energy barrier of Fig. 3, previously identified with the breaking of the ethylene's double bond. Thenceforth, this MO changes again, destabilizing and losing all trace of  $\pi^*$  character (see Fig. 4). At the last step of the reaction, the LUMO regains the antibonding Ti–alkyl nature, but now  $C_4$  replaces  $C_3$  and is the first carbon of the newly coordinated propyl chain.

In short the Ti–methyl bond is associated dominantly to the highest occupied MO, while the lowest unoccupied MO is essentially an antibonding orbital between  $C_3$  and the Ti site. Their bonding–antibonding character is an indication of the labile character of the methyl–Ti coordination bond. This explains why the methyl is easily displaced by the entrance of the ethylene. However, when the ethylene has entered the coordination sphere, the LUMO acquires a notable amount of  $\pi^*$  character, i. e., this bond is stabilized from +0.12 to –0.07 a. u. When the double bond has disappeared completely the original role of the HOMO and the LUMO is restored but now relating to the Ti–propyl bond.

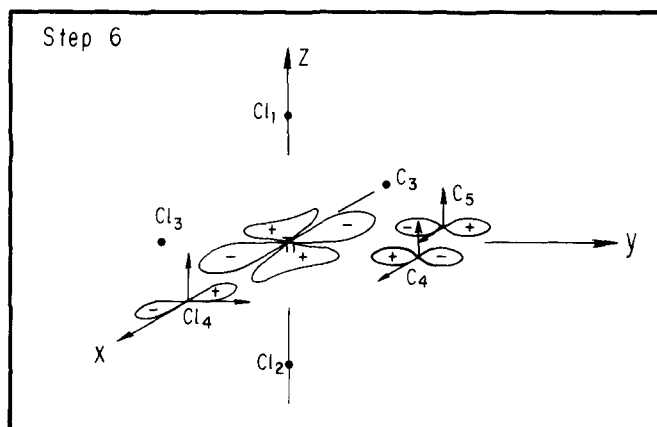


FIG. 6. Schematic representation of the atomic orbitals for the LUMO. Only an intermediate stage of the evolution is presented. The initial and final stages are similar to inserts (a) and (c) of Fig. 5 but with opposite signs for Ti contributions.

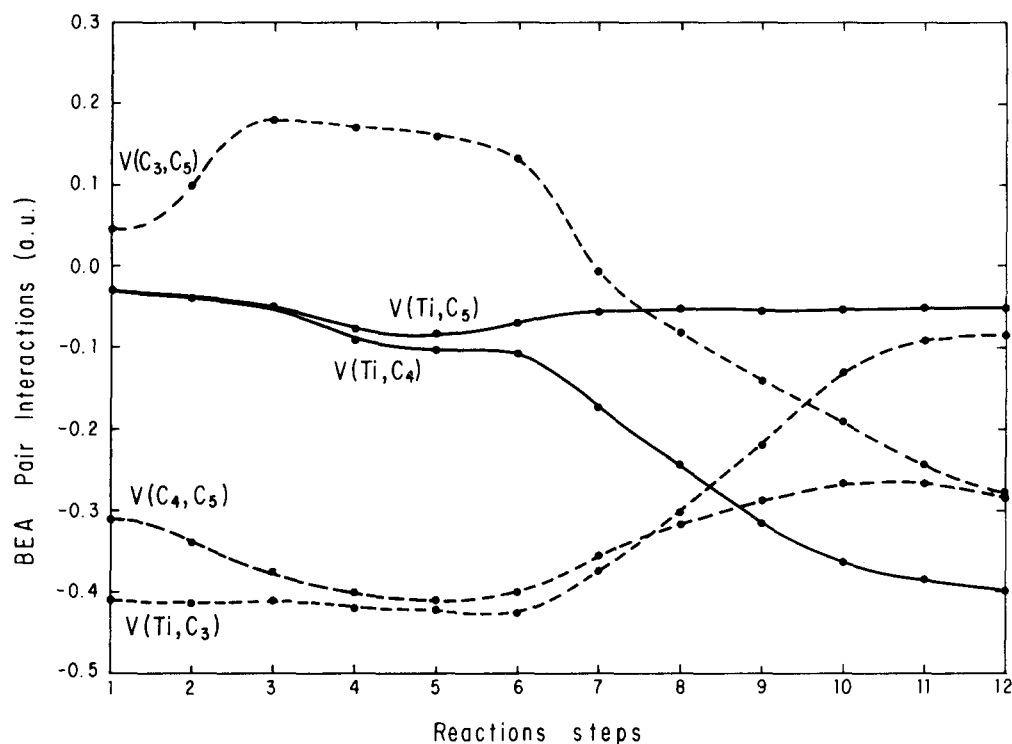


FIG. 7. Pairwise energies for selected BEA bonds as function of the reaction steps.

In closing, let us comment that the ethylene  $\pi$  bond follows an evolution somewhat similar but more involved than that of the  $\pi^*$  orbital. Table III emphasizes this evolution.

#### IV. BOND ENERGY ANALYSIS

The analysis of the system's total energy variations as well as the MO's evolution during the reaction proved to be basic to the understanding of the mechanism of the process within our model. However, it is supplementary and also interesting in itself to follow the dynamics *within each bond* or group of bonds, as is done in this section. It is convenient to note that the system wave function is defined up to a unitary transformation and, that no energy or electronic density partitioning associated with atoms (or groups of atoms) within a molecule is unique (Mulliken's electron population analysis<sup>10</sup> is an example). Bearing these limitations in mind, let us consider a partitioning of the total binding energy into pairwise interactions<sup>11</sup> as follows: total binding energy = total energy -  $\sum_A E(A) = \sum_{A \neq B} V(A, B)$ , where summations run over all atoms in a molecule,  $E(A)$  stands for the energy of atom  $A$  at infinity, and  $V(A, B)$  is related to the interaction between atoms  $A$  and  $B$ . Despite the two-center character of the  $V(A, B)$  energies, the traditional "bond energy" cannot be directly associated with these  $A-B$  interactions for two reasons: (i) In this *ab initio* study no correlation corrections were included, while in the common usage of bond energy the correlation comes in (see, for example, Pitzer<sup>12</sup>), and (ii) Whereas the total binding is usually obtained as the sum of the bond energies, in the bond energy analysis<sup>11</sup> (BEA) the binding energy is defined by the above equation, namely, by summing over *all*

the possible pairs of atoms in the system, attractive or repulsive. In the BEA language the  $V(A, B)$  are classified as "bonds" if they are negative and their absolute value is larger than a given threshold, and as "nonbonded interactions" otherwise.<sup>11</sup> We will use this terminology in what follows.

In Fig. 7 we present the BEA interactions for several pairs as they evolve during the reaction (a static description of the isolated catalyst is found in Appendix C). The Ti-C BEA interactions change little from steps 1 to 3, and represent a bond for the pair Ti-C<sub>3</sub> and two attractive interactions for the pairs Ti-C<sub>4</sub> and Ti-C<sub>5</sub>, respectively. But as soon as the ethylene coordinates with the Ti atom (steps 4-6), the nonbonded interactions  $V(\text{Ti}, \text{C}_5)$  and  $V(\text{Ti}, \text{C}_4)$  become more attractive, while the bond  $V(\text{Ti}, \text{C}_3)$  remains essentially unchanged in its energy. From step 6 on, a remarkably symmetric weakening of the  $V(\text{Ti}-\text{C}_3)$  bond and the formation of the Ti-C<sub>4</sub> bond is noteworthy, since this entire process proceeds with little energy loss. Concomitant to this binding mechanism, we have the transformation of the ethylene double bond into a single bond as well as a new bond formation, the C<sub>3</sub>-C<sub>5</sub> bond of the propyl chain. This is evidenced in Fig. 7: The  $V(\text{C}_4-\text{C}_5)$  bond is first stabilized (due to the ethylene coordination), then loses energy reaching a value substantially equal to that of the C<sub>3</sub>-C<sub>5</sub> single bond already formed at the last step of the reaction. The C<sub>4</sub>-C<sub>5</sub> bond breaking goes together with the  $V(\text{C}_3, \text{C}_5)$  changes. The  $V(\text{C}_3, \text{C}_5)$  of Fig. 7 shows an initial repulsion between the methyl and the ethylene during the latter's coordination (steps 1-5). After the ethylene coordination this repulsion begins to decrease. The new C<sub>3</sub>-C<sub>5</sub> bond is formed from step 8 on in agreement with the substantial lowering of the total energy in Fig. 3.

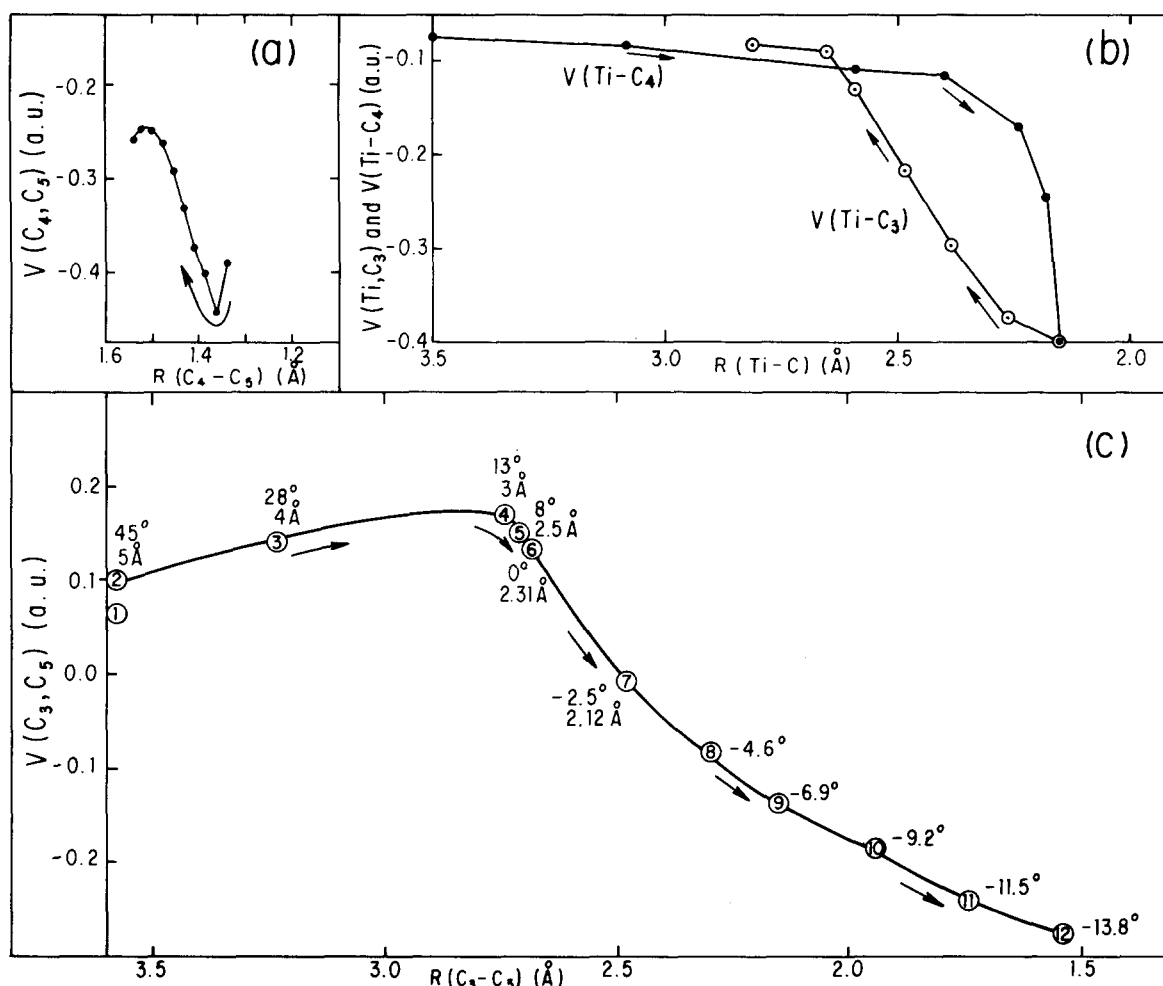


FIG. 8. Pairwise energies for selected BEA bonds as function of the corresponding internuclear distances.

All these binding mechanisms assume a somewhat different outlook if the BEA interactions are plotted as functions of the associated bond length, as done in Fig. 8. We must be aware, however, that the  $V(A, B)$  depend simultaneously on as many variables as the parameters were changed during the reaction (see Table I). In Fig. 8(a) the BEA interaction is reported for the carbon atoms in ethylene; the arrow indicates initial  $\rightarrow$  final steps of the process. The  $V(C_4, C_5)$  has a short range of variation during the reaction, going from 1.337 to 1.54 Å. During the ethylene coordination there is a small stabilization, then the bond loses its energy nearly regularly. From Fig. 8(b) we see that the  $Ti-C_3$  bond requires a longer stretching for breaking than the  $C_4-C_5$  bond. This long range character is interpreted as an indication of a rather ionic type of bond, which contrasts with the homopolar character of the  $\pi$  bond  $C_4-C_5$ . The  $V(Ti, C_4)$ , also plotted in Fig. 8(b), acquires the energy minimum at 2.15 Å, that is at exactly the same bond length and energy than the  $Ti-C_3$  bond in the first step of the reaction. The situation for the  $V(C_3, C_5)$  case is shown in Fig. 8(c), where for each point we provide the reaction step index. It is evident that the initial repulsion becomes an attraction after the activation barrier is surmounted.

Let us now consider a more general picture, the

group BEA, in which we analyze the binding energy within groups of atoms, rather than pairs of atoms. In this way, for each group we take into account not only the bonds  $V(A, B)$ , but also the nonbonded interactions, attractive or repulsive. The sum of the BEA interactions  $V(A, B)$  within a selected group of atoms yields the relative stability of that group, or self-energy. The sum of the pairwise interactions between atoms belonging to two groups gives the group-group interaction. In Fig. 9 we show the group BEA results for a few selected groups during the reaction process. The Ti and methyl as groups show a weak repulsion from the very beginning of the reaction that, in our model, will increase during the last part of the polymerization. The Ti and ethylene, as groups, show repulsion up to the ethylene coordination (step 6), and less so afterwards. Let us now analyse the catalyst and the ethylene as groups. By now we know that while at the beginning of the reaction the methyl and the ethylene are well defined chemical species, at the end they merge into the propyl which in turn can be singled out as a group. Thus, we have arbitrarily connected the two descriptions between steps 6 and 7. In this way, for the first six steps we report only the ethylene and catalyst self-energies,  $E(\text{ethylene})$  and  $E(\text{catalyst})$ , with their corresponding interaction,  $E(\text{ethylene, catalyst})$ . On the other hand, for the last six steps of the

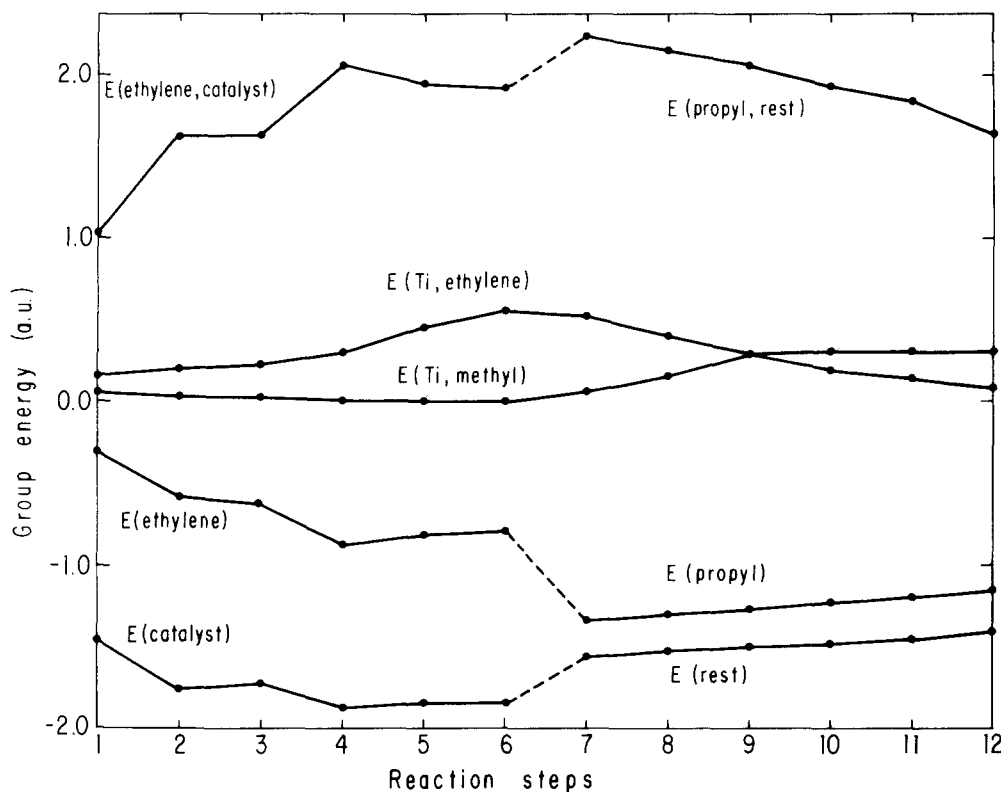


FIG. 9. Selected *group* BEA interactions as function of the reaction steps.

reaction, only the propyl self-energy  $E(\text{propyl})$  is reported in Fig. 9, as well as its interaction with what was left of the catalyst (denoted as “rest”). From these curves we learn that both ethylene and the catalyst become independently more stable at the expense of the closed shell–closed shell repulsion,  $E(\text{ethylene, catalyst})$ . This suggests that this negative–positive energy balance parallels the “charge back donation” of Ti proposed as an important concept to study catalytic reactions (see Sec. V).

All in all, by looking at Figs. 7 and 9 we may distinguish the following stages during the reaction: (1) From steps 1–5 there is mutual polarization as the *ethylene* coordinates at the catalyst site; (2) From steps 5–8 there appears a selective interaction of  $C_4$  with Ti and  $C_5$  and  $C_3$  concomitant to the  $\pi$  bond breaking in ethylene; and (3) After a transition state at steps 8 and 9 these new bonds are smoothly stabilized at the expense of the ones they replace (the double bond and the Ti–methyl bond) giving rise to the *formation of the propyl chain* (compare with Fig. 3).

## V. COMPARISON OF MODELS FOR THE CATALYTIC PROCESS AND SOME SPECULATIONS

As stated before, we consider the present study to be more of an “experiment” to establish whether *ab initio* techniques are of use to understand some general trends common to different catalytic processes than a complete analysis of a particular process. It is true that the model system studied, an aluminium–titanium complex acting for a chain growth reaction with ethylene as prime

reactant is clearly associated to the family of Ziegler–Natta catalytic processes. The nature of the model for the active site, however, was chosen so as to have some bearing in various systems. It may be considered as a selection of a molecular group on a solid catalyst surface, or related to “soluble catalyst” structures as the well known homogeneous catalyst formed by the reaction of one or two triethyl–aluminium molecules with Ti–cyclopentadienyl<sup>13</sup> or Ti–butoxy complexes.<sup>14</sup> We believe the results given in the previous sections might have relevance for these and other catalytic processes, keeping in mind, of course, the notable differences among the various chemical processes and the limitations that a theoretical model as this one inherently has. To explain these qualifications we will compare several traditional models with our results.

One of the first and finest attempts to relate the mechanism of this type of processes to a qualitative molecular orbital picture was the work of Cossee.<sup>3</sup> In it, the hypothesis is advanced of an octahedral complex in the Ti site with the alkyl chain in a *cis*-position to the coordinated ethylene. Cossee proposed the activation of the polymerization reaction (based on a tentative orbital scheme) arising from a back-donation effect. The latter is supposed to occur through a  $\sigma$  donation to the Ti–olefin bond from the ethylene  $\pi$  bond followed by a retrodonation to the ethylene  $\pi^*$  antibonding MO through the empty  $d$  orbitals of titanium.<sup>15</sup> This naturally implies a stabilization of one of the octahedral Ti complex  $t_{2g}$  orbitals. It is interesting to note that we indeed found an important stabilization for such an orbital (in

our case the  $d_{xy}$  function in Ti) whose energy was quite lower than that of the other (empty)  $d$  orbitals which in Table III were identified as MO's 75–78 with energies of +0.02 a.u. and higher.

Furthermore, it is well to recall that we did not study the Ti site with a rigid preconception of an octahedral structure with a vacant site. In fact, we have shown that the complex originally has a trigonal bipyramidal symmetry (see Appendix B). When the ethylene enters the coordination sphere, however, the alkyl moves to keep the total energy as low as possible. It moves in such a manner that when the coordination minimum is achieved (steps 4 and 5), they are effectively in positions quite close to an octahedral arrangement (see Fig. 2, step 5). The ethylene interaction does indeed stabilize the Ti  $d_{xy}$  orbital (by about 0.11 a.u.). This latter, in turn, substantially interacts with the ethylene  $\pi^*$  MO, as was shown in the discussion of the LUMO in Sec. III.

More recently, a reinvestigation of Cossee's scheme was carried out by Armstrong, Perkins, and Stewart<sup>16</sup> using semiempirical MO methods (in the CNDO approximation). They find that the Ti–methyl bond is quite localized in the highest bonding orbital of the complex, with the metal atom's contribution having an almost pure  $d$  orbital character. Secondly, they conclude that the  $\text{Al}(\text{CH}_3)_2$  moiety is essentially inert interacting only with the Ti. They also state that the  $3d-\pi^*$  admixing is quite weak. This last conclusion was, however, not confirmed by a similar study by Novaro, Chow, and Magnouat<sup>17</sup> who found that the LUMO was stabilized substantially by the  $\pi^*-d$  participation, in accordance to Cossee's estimations and also with our *ab initio* results (see Sec. III). It should be noted that these two works,<sup>16,17</sup> while using the same CNDO method, studied different catalysts, although both belong to the family of homogeneous organometallic Ti catalytic complexes.

In our work, also, we find that the Ti–methyl bond is located at the HOMO. Both the Ti–methyl and the Ti–ethylene interactions have a notable Ti  $d$  function contribution, although the Ti 4s function also contributes. In our study the  $\text{Al}(\text{CH}_3)_2$  moiety not only interacts with the methyl [see the  $V(\text{Al}-\text{C}_3)$  contribution in Table VI], but even with the ethylene carbons at certain stages of the reaction (see also Table III). More generally, we comment that the traditional picture of singling out only a few molecular orbitals and atomic groups of the complex to describe the reaction appears an oversimplification.

One crucial quantum mechanical prediction outside the scope of semiempirical calculations is the behavior of the total energy. The present model is based primarily on the interpretation of the energy barrier of the reaction pathway as given in Fig. 3. The CNDO studies relied more heavily on information about MO energies and the total energy thereof was simply reported to be continuously stabilized throughout the process<sup>16,17</sup>. For comparison we calculated the present reaction coordinate within a CNDO approximation, and obtained an unrealistic lowering of the total energy (140 kcal/mol) with no relation whatsoever to the structure of Fig. 3.

One prediction of the CNDO studies<sup>16,17</sup> which is confirmed here, is that the reaction between the alkyl and the olefin is substantially a concerted motion of these two moieties. This has an indirect relation with some questions raised in the Ziegler–Natta polymerization process like the controversy<sup>18</sup> whether the chain growth comes from a *cis*-migration of the alkyl or an insertion of the olefin into the Ti–alkyl bond. This alternative does not imply a sharp distinction in a quantum mechanical sense because, as we have seen, it is the entrance of the olefin that initiates the alkyl migration, which, in turn, facilitates the olefin insertion.

One apparent contradiction between the Cossee scheme and the CNDO studies was the following. Chatt and Schaw had proposed that a certain critical energy must be given to the system to expel the alkyl group as a radical which then attaches the nearest carbon on the olefin<sup>19</sup>. Armstrong, Perkins, and Stewart,<sup>16</sup> on the other hand, maintain that at all stages of the chain growth reaction the alkyl and the ethylene remain bonded to the titanium, and hence no energy for bond breaking is necessary. While there is no trace in the *ab initio* results for any radical liberation, some qualifications of the character of the Ti–methyl bond are necessary. In Sec. IV the bond energy analysis clearly shows a bonding Ti–C<sub>3</sub> attraction. However, when the interaction of the Ti with the methyl as groups is considered (consequently including the Ti repulsive interactions with the hydrogens, see Fig. 9), it is rather clear that the latter, is not tightly attached to the site. This is quantum mechanical description of a labile bond, not breaking away but nevertheless permitting the methyl group to behave as a “trapped radical” capable of reacting readily with the ethylene without being expelled from the coordination sphere.

Now let us speculate about a real catalytic system, trying to extrapolate the information of our calculations. Although the molecular interactions occur basically at one or more “active sites” of finite dimensions, this concept, apart from its dubious geometrical and molecular characterization, is far from being a well established and universally accepted definition. Our choice for the structure of the complex can, of course, be challenged as not corresponding to the active site. Simply, we consider our choice as a tentative approach to represent relevant perturbations at the Ti site due to different molecular groups. Indeed we are reminded that our present calculations can also be related to the homogeneous catalyst, where the initial catalyst geometry is much less ambiguous and has been generally accepted to be quite similar to the geometry studied here.<sup>14</sup> On the other hand, the best-known homogeneous catalysts have other groups within the Ti–Al coordination sphere (e.g., cyclopentadienyls, oxiarlyls or oxialkyls) whose influence could also be of importance. Besides, there are families of such catalysts where a Ti forms bridged structures with two Al atoms. This again has an important effect on the catalytic activity, since these catalysts oligomerize rather than polymerize the ethylene. In Appendix C the BEA analysis suggests that, if Ti is surrounded by *four* Cl's bridged to *two* Al, all groups would be less strongly coordinated at the Ti

TABLE IV. The Gaussian basis sets used in this study.

Ti (11s, 5p, 2d)		Cl (9s, 5p)		Al (9s, 5p)		C (7s, 3p)		
Exp.	Coeff.	Exp.	Coeff.	Exp.	Coeff.	Exp.	Coeff.	
	18 576.0	0.008209	13 360.94112	0.004241	3528.82063	0.0106673	1267.183972	0.005446
	1873.13	0.060952	1949.68227	0.032900	570.690937	0.0670285	190.603978	0.040526
1s	421.896	0.261875	444.161761	0.149519	149.74054	0.2278593	43.247698	0.179789
	116.872	0.540007	125.568229	0.424830	48.263778	0.4613234	11.964903	0.460002
	36.1981	0.280438	38.931568	0.519568	16.923777	0.3741655	3.663116	0.444594
2s	16.078015	0.363839	8.566727	0.255010	3.741587	0.4100390	0.539158	0.504860
	5.90144	0.676081	3.224050	0.775838	1.337578	0.6340241	0.16713	0.613125
3s	1.471891	0.359373	0.596934	0.378658	0.199651	0.3907024	4.187345	0.111922
	0.622027	0.670613	0.232767	0.657607	0.078399	0.6455438	0.854053	0.465078
4s	0.072885	0.563065	69.043766	0.093125	38.030333	0.0870360	0.19977	0.623756
	0.030973	0.469396	16.462889	0.410272	7.912971	0.4281252	H (3s)	
	154.363562	0.073124	4.672286	0.651931	1.914341	0.6640245	4.5018	0.070452
2p	35.045068	0.386685	1.127666	0.275218	0.2	0.4248636	0.68144	0.407826
	10.010682	0.682910	0.278734	0.817785	0.07	0.6498862	0.1514	0.647752
3p	2.596318	0.299563						
	0.765885	0.780367						
3d	2.919275	0.378378						
	0.582590	0.800506						

site. This would be a possible qualitative explanation for the high rate constant of the chain liberation in such catalysts.<sup>14</sup>

Going back to the heterogeneous catalyst, it would be desirable to perform additional studies on alternative models for the active site for example by considering other substituents at the Ti coordination sphere. In particular, the study of how the presence of more than one Ti atom affects the process would be quite interesting. To further emphasize this interest let us make a few speculations thereupon. If the molecular orbital structure is not dramatically different from the one discussed above when another Ti atom is considered, we can guess that its main effect will be to donate electrons towards the active site. The large positive charge on the metal atoms, specially Ti, reported in Sec. II would support this. Also, the fact that the additional Ti would bring one more valence electron to the system (as compared with an Al neighbor) implies the possibility of such electron-migration. Where to? The LUMO is energetically very stable (see Fig. 4) and therefore one would expect that the presence of a *d* electron donating metal, (coordinated to the Ti site) could greatly facilitate both the methyl migration and the  $\pi$  bond breaking. Indeed the lowest unoccupied MO causes the Ti-methyl bond to be labile and later stabilizes while acquiring the character of an ethylene's  $\pi^*$  orbital when this molecule is coordinated. This would perhaps enhance the reaction both facilitating the alkyl movement and helping effectively to weaken the double bond. This and other questions should perhaps be addressed to in future *ab initio* studies of the catalysis phenomenon.

## VI. CONCLUDING REMARKS

For the first time, perhaps, an *ab initio* study of the evolution of a catalyzed reaction including a realistic model for the catalyst has been given. However, our description of the ethylene polymerization could perhaps be improved for example by performing a number of

variations of the parameters defining the multidimensional potential energy surface for the 24 center, 146 electron system.

The most valuable result of this type of calculation is the evolution of the total energy through the reaction coordinate. Keeping in mind the high cost of the computation, we think it is necessary to try some approximate techniques which, however, would prove sufficiently trustworthy for energy predictions. For this reason we are presently considering the use of a pseudopotential approximation.<sup>20,21</sup> The results of this work will provide quantitative test for such calculations.<sup>22</sup>

In closing we would like to comment, from a purely theoretical point of view, that even for such a complex problem as this one (considering not only the dimensions of the system but also its evolution), quantum mechanics gives a cogent picture and useful information reflecting the catalytic phenomena, even if entropic effects have not been considered at all.

As concerns the relation with practical problems of catalysis, in Sec. V we have engaged in some speculations on how some changes in the structure of the reactive site might lead to alternative views on the catalytic process. If a substantial number of studies of this type would exist, perhaps some hope for the theoretical prediction of certain features of new catalysts could be raised. On the other hand, one must be very conscious that at the present moment of the art-science of catalysis theory cannot replace experiment, and perhaps never will. A valuable enough byproduct of such studies would be just to interest the catalysis chemist to orient his experiments to produce a more fruitful and continuous dialogue with the theoretician, a link so sorely needed in this field.

## ACKNOWLEDGMENTS

We would like to thank Professor P. Pino (Polytechnic Institute, Zurich) and Dr. M. Berrondo (UNAM) for

TABLE V. Variation of some relevant parameters defining the geometry of the catalytic complex. All  $\Delta E$  are referred to the energy of step 1 in Table I in text, with the exception of those of entry 1. A titanium–methyl bond distance of 2.15 Å was held constant during all the variations (see Ref. 5).

Entries for the parameter variations	Methyl parameters		Ethylene parameters			Energy changes $\Delta E$ (kcal/mol)
	$\alpha_R$	$\alpha_T$	$\alpha_0$	$\alpha_I$	$r(\text{Å})$	
(1) Variations of $\alpha_R$ for the catalyst alone (before the entrance of $C_2H_4$ )	45°	0	...	...	...	Reference value
	28	0	...	...	...	+1.7 <sup>a</sup>
	13	0	...	...	...	+5.8 <sup>a</sup>
	0	0	...	...	...	+18.3 <sup>a</sup>
(2) Variation of $\alpha_R$ when ethylene approaches at $R=4.0$ Å	45	0	0	117	1.337	+8.3 <sup>a</sup>
	35	0	0	117	1.337	-0.8 <sup>a</sup>
	28	0	0	117	1.337	-1.9 <sup>a</sup>
	20	0	0	117	1.337	-1.0 <sup>a</sup>
(3) Variation of $\alpha_R$ $R=3.0$ Å	28	0	16	116	1.360	+2.3 <sup>a</sup>
	20	0	16	116	1.360	-3.0 <sup>a</sup>
	13	0	16	116	1.360	-7.3 <sup>a</sup>
	0	0	16	116	1.360	-4.6 <sup>a</sup>
(4) Variation of $\alpha_R$ $R=2.5$ Å	13	0	16	115	1.383	-1.9 <sup>a</sup>
	4	0	16	115	1.383	-4.7 <sup>a</sup>
	0	0	16	115	1.383	-4.0 <sup>a</sup>
(5) Variation of $\alpha_T$ $R=3.0$ Å	28	-30	8	116	1.360	+35.2
	28	0	8	116	1.360	+17.0
	28	60	8	116	1.360	+53.2
(6) Variation of $\alpha_0$ $R=2.5$ Å	13	0	10	115	1.383	-0.1
	13	0	16	115	1.383	+0.9
	13	0	22	115	1.383	+3.5
(7) Variation of $\alpha_I$ $R=2.5$ Å	13	0	16	114	1.383	+1.1
	13	0	16	115	1.383	+0.9
	13	0	16	116	1.383	+0.8
(8) Variation of $r$ $R=2.5$ Å	13	0	16	115	1.337	+2.5
	13	0	16	115	1.383	+0.9
	13	0	16	115	1.429	+2.6

<sup>a</sup>These numbers were obtained from a Univac 1000/10 computer, all others are from the IBM 370/168 using the same IBMOL program.

critical reading of the manuscript and to Dr. G. Corongiu for her invaluable help with practical aspects of the computations carried out in Novara. One of us (EC) wishes to acknowledge the hospitality of the UNAM staff during his stay in Mexico. We acknowledge the staff of Datamont and Dualdata for their collaboration.

#### APPENDIX A: ATOMIC GAUSSIAN BASIS SET

The atomic Gaussian basis set used in this study with the contraction scheme is reported in Table IV.

#### APPENDIX B: GEOMETRIC PARAMETERS OF THE CATALYTIC COMPLEX

A schematic representation of the catalytic complex and the reactant geometries were given in the text, Fig. 1. For the isolated catalyst a quasitrigonal bipyramidal structure with bond lengths and internal angles taken mostly from experimental values (see Ref. 5), has been tested and shown to be the minimal energy configuration (see entry 1 in Table V). Attention will be focused here upon the variation of the most relevant geometrical parameters of the complex when the ethylene is entering the titanium coordination sphere, Fig. 10. The listing of parameters defining the molecular

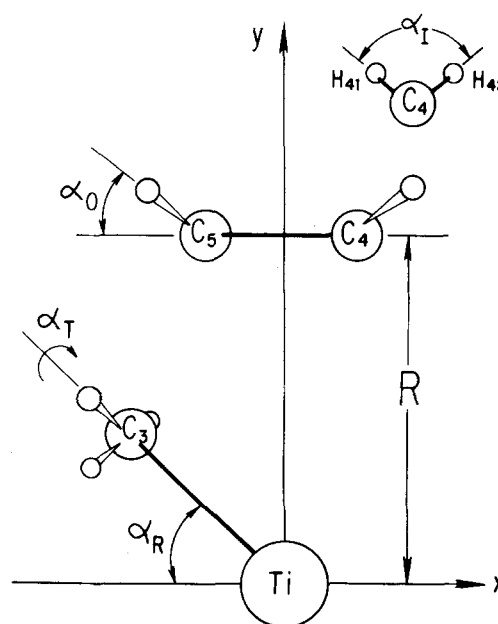


FIG. 10. Geometrical parameters varied as described in the text.

TABLE VI. Pairwise interactions within the isolated catalyst. All energies are given in atomic units.

Bonds		Nonbonded Interactions					
Pair	Energy	Attractive		Repulsive			
		Pair	Energy	Pair	Energy	Pairs	Energies
Al-C <sub>1</sub>	-0.419	Ti-C <sub>1</sub>	-0.106	Al-Ti	0.686	Hydrogens within the methyl	0.09
Al-C <sub>2</sub>	-0.419	Ti-C <sub>2</sub>	-0.106	C <sub>1</sub> -C <sub>2</sub>	0.297	Carbons in any of the methyls with Cl's	0.08
C <sub>1</sub> -H <sub>11</sub>	-0.365	Al-Cl <sub>1</sub>	-0.071	Al-H <sub>14</sub>	0.189		
C <sub>1</sub> -H <sub>12</sub>	-0.355	Al-Cl <sub>2</sub>	-0.071	Al-H <sub>12</sub>	0.168		
C <sub>1</sub> -H <sub>13</sub>	-0.355	Al-C <sub>3</sub>	-0.062	Al-H <sub>13</sub>	0.168	Hydrogens within end methyls	0.07
C <sub>2</sub> -H <sub>21</sub>	-0.355	C <sub>1</sub> -H <sub>21</sub>	-0.010	Al-H <sub>21</sub>	0.189		
C <sub>2</sub> -H <sub>22</sub>	-0.355	C <sub>1</sub> -H <sub>22</sub>	-0.009	Al-H <sub>22</sub>	0.168	Hydrogens within end methyls with Ti	0.05
C <sub>2</sub> -H <sub>23</sub>	-0.355	C <sub>1</sub> -H <sub>23</sub>	-0.009	Ti-H <sub>23</sub>	0.168		
C <sub>3</sub> -H <sub>31</sub>	-0.328	C <sub>2</sub> -H <sub>11</sub>	-0.010	Ti-H <sub>31</sub>	0.156		
C <sub>3</sub> -H <sub>32</sub>	-0.338	C <sub>2</sub> -H <sub>12</sub>	-0.009	Ti-H <sub>32</sub>	0.159	Cl's bridged with Z axis Cl's	0.05
C <sub>3</sub> -H <sub>33</sub>	-0.338	C <sub>2</sub> -H <sub>13</sub>	-0.009	Ti-H <sub>33</sub>	0.159		
Al-Cl <sub>3</sub>	-0.330	Cl <sub>2</sub> -H <sub>32</sub>	-0.010	C <sub>3</sub> -Cl <sub>1</sub>	0.132	Cl <sub>3</sub> -Cl <sub>4</sub>	0.04
Al-Cl <sub>4</sub>	-0.331	Cl <sub>1</sub> -H <sub>33</sub>	-0.010	C <sub>3</sub> -Cl <sub>2</sub>	0.132		
Ti-Cl <sub>1</sub>	-0.354			C <sub>1</sub> -C <sub>3</sub>	0.117	Cl <sub>1</sub> -Cl <sub>2</sub>	0.03
Ti-Cl <sub>2</sub>	-0.354			C <sub>2</sub> -C <sub>3</sub>	0.117	Methyl's hydrogens with Al	0.02
Ti-C <sub>3</sub>	-0.384						
Ti-Cl <sub>3</sub>	-0.253						
Ti-Cl <sub>4</sub>	-0.253						

configurations as well as the latter total energies are summarized in Table V.

Two angles  $\alpha_T$  and  $\alpha_R$  position the methyl group bound to Ti,  $\alpha_T$  being associated to a torsional motion of the hydrogens about the Ti-C<sub>3</sub> bond and  $\alpha_R$  indicating a rotation in the  $xy$  plane of the alkyl group towards the ( $-x$ ) axis. As shown by entries 2-5 in Table V, the changes of the torsional angle from the 0° value cost energy to the system, whereas a diminution of  $\alpha_R$  re-

sults in a favorable energy balance. Thus, in the first stages of the reaction two features are worth to be noted: (i) As any transfer of energy from the torsional mode to the system is excluded, this mode can be considered as inactive; (ii) the ease of the methyl to rotate in the plane  $xy$  when the ethylene is present, is an indication of the labile character of the Ti-C<sub>3</sub> bond. In that sense, the planar rotation pictured by  $\alpha_R$  may be considered as an active mode. All in all this analysis suggests that at the beginning of the reaction a concerted

TABLE VII. Group energies for seven possible ways of grouping atoms within the catalytic complex  $TiCl_4 \cdot Al(CH_3)_3$ . All energies are given in atomic units.

(a)	Methyl	End methyl	Complex without the 3 methyls	(b)	Ti+Cl bridges	Complex without Ti and Cl bridges	Ti+z axis Cl's	Complex without Ti and z axis Cl's
Methyl	-0.738			Ti+Cl <sup>-</sup> bridges	-0.467			
End methyl	0.108	-0.849		Complex without Ti and Cl bridges	0.092	-1.399		
Complex without the 3 methyls	0.426	0.406	-1.056	Ti+z axis Cl's			-0.678	
				Complex without Ti and z axis Cl's			-0.859	-1.956

motion of the methyl and ethylene takes place: i. e., while the incoming ethylene penetrates the Ti coordination sphere, the methyl rotates towards the  $(-x)$  axis. Thus the complex acquires a quasioctahedral structure as the ethylene enters the coordination sphere. It is important to notice however, that the minimal energy pathway, depicted in entries 2–4 in Table V, implies a relation between the methyl movement and the ethylene's entrance, i. e.,  $\alpha_R$  and  $R$  have to be changed simultaneously to allow the energy lowering from the latter's coordination. Actually, from the results of Table V (entries 2–4), the different choices for  $\alpha_R$  give the potential energy surface the appearance of a deep gorge with steep walls.

Three parameters were used to indicate the geometrical changes of the reacting ethylene during the process:  $\alpha_0$ , the orientation angle indicating how much the ethylene hydrogens go out of the original molecular plane;  $\alpha_I$ , the internal angle among any of the two hydrogen pairs bonded to a carbon; and  $r$ , the C–C bond length. Entries 6–8 in Table V show the energy changes in the system when these parameters are varied away from the isolated ethylene ones ( $\alpha_0 = 0^\circ$ ,  $\alpha_I = 117^\circ$ ,  $r = 1.337 \text{ \AA}$ ). In general, these variations are not very expensive energetically. Notice, however, that the C–C distance  $r$  has an energy minimum at a distance slightly larger than in the isolated ethylene molecule. This is an indication that although the Ti–ethylene interaction changes the ethylene's original structure the change is not dramatic.

### APPENDIX C: BOND ENERGY ANALYSIS

Certain insight of the catalytic functions of the titanium–aluminium complex can be obtained when the bond energy analysis is performed on the *isolated catalyst* calculation. The latter's total energy was reported elsewhere<sup>5</sup> as well as the molecular orbital information,<sup>9</sup> but a detailed BEA study was not yet presented.

Table VI gives the pairwise interactions within the isolated catalyst. Attractions smaller than  $-0.01$  and repulsions of less than  $0.02$  a. u. are not reported in this table. In the last two columns, repulsions smaller than  $0.1$  a. u. are grouped and rounded off. We notice that the rather strong Ti–C<sub>1</sub> and Ti–C<sub>2</sub> nonbonded attractions are balanced by the repulsion between Ti and the end–methyl hydrogens. Therefore, the net interaction between the metal at the active site and the end–methyl groups is small. However, the pairwise energy between the Al and the two  $z$  axis chlorines and between Al and the methyl carbon are substantially large. Thus, the aluminium, even though not being at the active site, certainly plays an specific role.

In Table VII the group BEA data are reported for seven ways of grouping atoms within the isolated catalyst. The group self-energies are given onto the diagonal, while the off-diagonal elements represent the group–group interactions. From entry (a) of this table, we learn that the methyl is *less stable* than any one of the two end methyls. This information supplemented with that of Table VI (the Al–C bond is stronger than the Ti–C bond) leads us to the conclusion that in the complex the methyl is *loosely bonded* vis-a-vis the end methyls. Thus, the methyl is a labile, highly reactive group. The four rows in entry (b) of Table VII distinguish the role of the chlorine atoms in the complex. It is worth to note the small repulsion between the group (Ti+ chlorine bridges) with the rest of the catalyst, in contrast with the strong repulsion between the group (Ti+  $z$  axis chlorines) with the rest. This brings up the suggestion that either substitution of Al by another atom or the bridges by another structure could affect the role of the complex in a reaction (see Sec. V).

- <sup>1</sup>K. Ziegler, E. Holzkamp, H. Breil and H. Martin, *Angew. Chem.* **67**, 541 (1955).
- <sup>2</sup>G. Natta, *Macromol. Chem.* **16**, 213 (1955).
- <sup>3</sup>P. Cossee, *J. Catal.* **16**, 213 (1964).
- <sup>4</sup>E. Clementi and J. Mehl, *IBM Res. J.* 833 (1971).
- <sup>5</sup>G. Giunchi, E. Clementi, M. E. Ruiz-Vizcaya, and O. Novaro, *Chem. Phys. Lett.* **49**, 8 (1977).
- <sup>6</sup>G. Natta and I. Pasquon, *Adv. Catal.* **11**, 1 (1959).
- <sup>7</sup>J. P. Machon, R. Hermant, and J. P. Houzeaux, *J. Polym. Sci. Symp.* **52**, 107 (1975).
- <sup>8</sup>J. C. W. Chien, *J. Am. Chem. Soc.* **81**, 86 (1959).
- <sup>9</sup>FUNAM Internal Report (1977).
- <sup>10</sup>R. W. Mulliken, *J. Chem. Phys.* **23**, 1833, 1841, 2338, 2343 (1955).
- <sup>11</sup>E. Clementi, *Lecture Notes in Chemistry*, Vol. 2 (Springer-Verlag, 1977); *Bull. Soc. Chim. Belg.* **85**, 969 (1976).
- <sup>12</sup>K. S. Pitzer, *Quantum Chemistry* (Prentice-Hall, New York, 1953), p. 170.
- <sup>13</sup>G. Natta, P. Pino, G. Mazzanti, V. Giannini, E. Mantica, and M. Peraldo, *Chim. Ind. (Milan)* **39**, 19 (1957).
- <sup>14</sup>G. Henrici-Olivé and S. Olivé, *J. Polym. Sci. Polym. Lett. Ed.* **12**, 39 (1974); O. Novaro, S. Chow, and Ph. Magnouat, *J. Polym. Sci. Polym. Lett. Ed.* **13**, 761 (1975).
- <sup>15</sup>J. Chatt and L. A. Duncanson, *J. Chem. Soc.* 2939 (1953).
- <sup>16</sup>D. R. Armstrong, P. G. Perkins, and J. P. Stewart, *J. Chem. Soc. (Dalton)* 1972 (1972).
- <sup>17</sup>O. Novaro, S. Chow, and P. Magnouat, *J. Catal.* **41**, 91 (1976).
- <sup>18</sup>G. Henrici-Olivé and S. Olivé, *Angew. Chem.* **10**, 105 (1971).
- <sup>19</sup>J. Chatt and B. L. Shaw, *J. Chem. Soc.* 705 (1959).
- <sup>20</sup>J. C. Barthelat, P. Durand, and A. Serafini, *Mol. Phys.* **33**, 159 (1977).
- <sup>21</sup>Ch. Teichtel, J. P. Malrieu, and J. C. Barthelat, *Mol. Phys.* **33**, 181 (1977).
- <sup>22</sup>Work in progress.